PTEP

Prog. Theor. Exp. Phys. **2019**, 113B04 (16 pages)
DOI: 10.1093/ptep/ptz119

Fermion mass and mixing in a low-scale seesaw model based on the S_4 flavor symmetry

V. V. Vien[1,2,*], H. N. Long[3,4,*], and A. E. Cárcamo Hernández[5]

[1]*Theoretical Particle Physics and Cosmology Research Group, Advanced Institute of Materials Science, Ton Duc Thang University, Ho Chi Minh City 700000, Vietnam*
[2]*Faculty of Applied Sciences, Ton Duc Thang University, Ho Chi Minh City 700000, Vietnam*
[3]*Institute of Physics, VAST, 10 Dao Tan, Ba Dinh, Hanoi 100000, Vietnam*
[4]*Bogoliubov Laboratory for Theoretical Physics, Joint Institute for Nuclear Researches, 141980 Dubna, Moscow Region, Russia*
[5]*Universidad Técnica Federico Santa María and Centro Científico-Tecnológico de Valparaíso, Casilla 110-V, Valparaíso, Chile*
*E-mail: vovanvien@tdtu.edu.vn, hnlong@iop.vast.ac.vn, antonio.carcamo@usm.cl

Received June 11, 2019; Revised September 4, 2019; Accepted September 19, 2019; Published November 21, 2019

We construct a low-scale seesaw model to generate the masses of active neutrinos based on S_4 flavor symmetry supplemented by the $Z_2 \times Z_3 \times Z_4 \times Z_{14} \times U(1)_L$ group, capable of reproducing the low-energy Standard Model (SM) fermion flavor data. The masses of the SM fermions and the fermionic mixing parameters are generated from a Froggatt–Nielsen mechanism after spontaneous breaking of the $S_4 \times Z_2 \times Z_3 \times Z_4 \times Z_{14} \times U(1)_L$ group. The obtained values for the physical observables of the quark and lepton sectors are in good agreement with the most recent experimental data. The leptonic Dirac CP-violating phase $\delta_{\rm CP}$ is predicted to be 259.579° and the predictions for the absolute neutrino masses in the model can also saturate the recent constraints.

Subject Index B40, B54, B55, B57

1. Introduction

Despite its great success, the Standard Model (SM) still has serious drawbacks such as the lack of mechanisms that explain the smallness of neutrino masses, the large hierarchy of charged fermion masses, the fermionic mixing angles, the leptonic CP violation, etc. Another puzzle of the SM is that it does not explain why there are three generations of fermions. This puzzle can be addressed in the 3-3-1 models (see Ref. [1] and references therein). Hence, the neutrino masses and lepton mixings can be regarded as one of the most important pieces of evidence of physics beyond the SM. Among the possible extensions of the SM, discrete symmetries associated with the SM extensions are an useful tool to explain the observed pattern of SM fermion masses and mixing angles. According to the neutrino oscillation experimental data [2], the best-fit values of neutrino mass squared differences and the leptonic mixing angles are

$$\begin{aligned}
&\sin^2(\theta_{12}) = 0.307 \pm 0.013, \quad \sin^2(\theta_{13}) = (2.18 \pm 0.07) \times 10^{-2}, \\
&\sin^2(\theta_{23}) = 0.536^{+0.023}_{-0.028} \quad \text{(Inverted order)}, \\
&\sin^2(\theta_{23}) = 0.512^{+0.019}_{-0.022} \quad \text{(Normal order, octant I)}, \\
&\sin^2(\theta_{23}) = 0.542^{+0.019}_{-0.022} \quad \text{(Normal order, octant II)},
\end{aligned} \tag{1}$$

Funded by SCOAP[3]

$$\Delta m^2_{21} = (7.53 \pm 0.18) \times 10^{-5}\,\text{eV}^2,$$
$$\Delta m^2_{32} = (-2.53 \pm 0.05) \times 10^{-3}\,\text{eV}^2 \ (S = 1.2) \ \text{(Inverted order)},$$
$$\Delta m^2_{32} = (2.444 \pm 0.034) \times 10^{-3}\,\text{eV}^2 \qquad \text{(Normal order)}.$$

The large leptonic mixing angles given in Eq. (1) are completely different from the quark mixing ones defined by the Cabibbo–Kobayashi–Maskawa (CKM) matrix [3,4] and this has stimulated works on flavor symmetries.

One of the simplest possibilities to understand small non-zero neutrino masses is probably the seesaw mechanism, including types I, II, III and/or their combinations, which has been briefly reviewed in Ref. [5]. However, in these scenarios, the scale of the masses of the right-handed neutrinos should be very high; this cannot be reached in the near future. In the inverse and linear seesaw mechanism [6–28] the small neutrino masses arise as a result of new physics at the TeV scale, which may be probed in the Large Hadron Collider (LHC) experiments. In such low-scale models, both renormalizable and non-renormalizable interactions are included, which can explain the fermion masses and mixings. In the basis (ν, N, S), the neutrino mass matrix can be presented in the form of a 3×3 block matrix where each element is a submatrix. Depending on the position of the zero elements in the mass matrix, active neutrinos can receive masses through inverse or/and linear seesaw mechanisms that all require some elements of the mass matrix to be zero or very small and none of them are forbidden by the SM symmetry; however, such terms can be avoided by introducing additional flavor symmetries.

In this paper we propose the possibility of predicting fermion masses and mixing angles in the framework of the low-scale seesaw mechanism with S_4 flavor symmetry. S_4 is the permutation group of four objects, which is also the symmetry group of a cube. It has 24 elements divided into 5 conjugacy classes, with $\underline{1}, \underline{1}', \underline{2}, \underline{3}$, and $\underline{3}'$ as its 5 irreducible representations. We will work in the basis in which $\underline{3}, \underline{3}'$ are real representations whereas $\underline{2}$ is complex. For the Clebsch–Gordan coefficients of the S_4 group see, for instance, Ref. [29].

The content of this paper is as follows. In Sect. 2 we present the necessary elements of the linear seesaw model under the S_4 symmetry and introduce the necessary Higgs fields responsible for fermion masses and mixings. Section 3 deals with quark masses and mixings and Sect. 4 is devoted to lepton masses and mixings. We conclude in Sect. 5.

2. The model

We consider a three Higgs doublet model with several gauge singlet scalars, where the SM gauge symmetry is supplemented by the $S_4 \times Z_2 \times Z_3 \times Z_4 \times Z_{14} \times U(1)_L$ group. In this work, three left-handed leptons ψ_L and three right-handed neutrinos ν_R as well as extra neural leptons N_L, N_R, S_L, S_R are each put in one S_4 triplet while the first right-handed charged lepton l_{1R} and the last two right-handed charged leptons $l_{2,3R}$ transform as $\underline{1}$ and $\underline{2}$ under S_4 symmetry, respectively. For the quark sectors, all the families q_{1L}, u_{1R}, d_{1R} are put in $\underline{1}'$ and $q_{2L}, q_{3L}, u_{2R}, u_{3R}, d_{2R}, d_{3R}$ transform as $\underline{1}$ under S_4. The particle spectrum of our model and their assignments under the $SU(2)_L \times U(1)_L \times S_4 \times Z_2 \times Z_3 \times Z_4 \times Z_{14}$ group is summarized in Tables 1 and 3 where the numbered subscripts on fields in order define components of their S_4 multiplet representations as well as the quantum numbers corresponding to other groups of the model. We use the S_4 discrete group since it is the smallest non-Abelian discrete group having irreducible triplet and doublet representations. The discrete group S_4 is crucial to get a predictive fermion sector consistent with the low-energy fermion flavor data.

Table 1. $SU(2)_L \times U(1)_L \times S_4 \times Z_2 \times Z_3 \times Z_4 \times Z_{14}$ assignments for quarks and scalars.

	q_{1L}	q_{2L}	q_{3L}	u_{1R}	u_{2R}	u_{3R}	d_{1R}	d_{2R}	d_{3R}	H	H'	H''	χ
$SU(2)_L$	2	2	2	1	1	1	1	1	1	2	2	2	1
$U(1)_L$	0	0	0	0	0	0	0	0	0	0	0	0	0
S_4	$\underline{1}'$	$\underline{1}$	$\underline{1}$	$\underline{1}'$	$\underline{1}$	$\underline{1}$	$\underline{1}'$	$\underline{1}$	$\underline{1}$	$\underline{1}$	$\underline{1}'$	$\underline{1}$	$\underline{1}$
Z_2	1	1	1	-1	-1	-1	1	1	1	-1	-1	1	1
Z_3	1	1	1	1	1	1	1	1	1	1	1	1	1
Z_4	1	1	1	1	1	1	1	1	1	1	1	1	1
Z_{14}	$e^{-\frac{3i\pi}{7}}$	$e^{-\frac{2i\pi}{7}}$	1	$e^{\frac{3i\pi}{7}}$	$e^{\frac{2i\pi}{7}}$	1	$e^{\frac{5i\pi}{7}}$	$e^{\frac{3i\pi}{7}}$	$e^{\frac{3i\pi}{7}}$	1	1	1	$e^{-\frac{i\pi}{7}}$

Extra symmetries Z_2, Z_3, Z_4, and Z_{14} are additionally introduced in order to get the desired structure of the fermion mass matrices, which will be discussed in detail in Sect. 4.

3. Quark masses and mixings

The quark contents and the corresponding scalar fields of the model, under $[SU(2)_L, U(1)_L, S_4, Z_2, Z_3, Z_4, Z_{14}]$, are given in Table 1.

The quark Yukawa terms invariant under the symmetries of the model under consideration take the form:

$$\begin{aligned}
\mathcal{L}_Y^{(q)} = {} & y_{11}^{(u)}\overline{q}_{1L}\widetilde{H}u_{1R}\frac{\chi^6}{\Lambda^6} + y_{12}^{(u)}\overline{q}_{1L}\widetilde{H'}u_{2R}\frac{\chi^5}{\Lambda^5} + y_{13}^{(u)}\overline{q}_{1L}\widetilde{H'}u_{3R}\frac{\chi^3}{\Lambda^3} \\
& + y_{21}^{(u)}\overline{q}_{2L}\widetilde{H'}u_{1R}\frac{\chi^5}{\Lambda^5} + y_{22}^{(u)}\overline{q}_{2L}\widetilde{H}u_{2R}\frac{\chi^4}{\Lambda^4} + y_{23}^{(u)}\overline{q}_{2L}\widetilde{H}u_{3R}\frac{\chi^2}{\Lambda^2} \\
& + y_{31}^{(u)}\overline{q}_{3L}\widetilde{H'}u_{1R}\frac{\chi^3}{\Lambda^3} + y_{32}^{(u)}\overline{q}_{3L}\widetilde{H}u_{2R}\frac{\chi^2}{\Lambda^2} + y_{33}^{(u)}\overline{q}_{3L}\widetilde{H}u_{3R} \\
& + y_{11}^{(d)}\overline{q}_{1L}H''d_{1R}\frac{\chi^7}{\Lambda^7} + y_{22}^{(d)}\overline{q}_{2L}H''d_{2R}\frac{\chi^5}{\Lambda^5} + y_{23}^{(d)}\overline{q}_{2L}H''d_{3R}\frac{\chi^5}{\Lambda^5} \\
& + y_{32}^{(d)}\overline{q}_{3L}H''d_{2R}\frac{\chi^3}{\Lambda^3} + y_{33}^{(d)}\overline{q}_{3L}H''d_{3R}\frac{\chi^3}{\Lambda^3} + \text{H.c.}
\end{aligned} \tag{2}$$

Note that the lightest of the physical neutral scalars states of H, H', H'' is the SM-like 125 GeV Higgs boson discovered at the LHC. As indicated by Eq. (2), the top quark mass mainly arises from the renormalizable quark Yukawa term involving H. Thus the SM-like 125 GeV Higgs predominantly arises from the CP-even neutral part of H. Furthermore, in view of the large amount of free and uncorrelated parameters of the low-energy scalar potential of the model, there is a lot of freedom to adjust the required pattern of scalar masses, thus allowing one to safely assume that the remaining scalars are heavy and outside the LHC's reach. In addition, the loop effects of the heavy scalars contributing to precision observables can be suppressed by making an appropriate choice of the free parameters in the scalar potential. These adjustments do not affect the physical observables in the quark and lepton sectors, which are determined mainly by the Yukawa couplings.

Assuming that the $SU(2)$ Higgs doublets H, H', H'' do acquire vacuum expectation values (VEVs) at the electroweak symmetry breaking scale $v = 246$ GeV and the gauge singlet scalar χ gets a VEV of the order of $\lambda\Lambda$, with $\lambda = 0.225$ being one of the Wolfenstein parameters and Λ the model cutoff,

Table 2. Model and experimental values of the quark masses and CKM parameters.

Observable	Model value	Experimental value
m_u (MeV)	1.11	$1.45^{+0.56}_{-0.45}$
m_c (MeV)	639	635 ± 86
m_t (GeV)	172.3	$172.1 \pm 0.6 \pm 0.9$
m_d (MeV)	2.9	$2.9^{+0.5}_{-0.4}$
m_s (MeV)	57.7	$57.7^{+16.8}_{-15.7}$
m_b (GeV)	2.82	$2.82^{+0.09}_{-0.04}$
$\sin\theta_{12}^{(q)}$	0.225	0.225
$\sin\theta_{23}^{(q)}$	0.0421	0.0421
$\sin\theta_{13}^{(q)}$	0.003 65	0.003 65
J	3.18×10^{-5}	$(3.18 \pm 0.15) \times 10^{-5}$

we find that the SM quark mass matrices are given by:

$$M_U = \begin{pmatrix} a_{11}^{(u)}\lambda^6 & a_{12}^{(u)}\lambda^5 & a_{13}^{(u)}\lambda^3 \\ a_{12}^{(u)}\lambda^5 & a_{22}^{(u)}\lambda^4 & a_{23}^{(u)}\lambda^2 \\ a_{13}^{(u)}\lambda^3 & a_{23}^{(u)}\lambda^2 & a_{33}^{(u)} \end{pmatrix} \frac{v}{\sqrt{2}}, \qquad M_D = \begin{pmatrix} a_{11}^{(d)}\lambda^7 & 0 & 0 \\ 0 & a_{22}^{(d)}\lambda^5 & a_{23}^{(d)}\lambda^5 \\ 0 & a_{32}^{(d)}\lambda^3 & a_{33}^{(d)}\lambda^3 \end{pmatrix} \frac{v}{\sqrt{2}},$$

where

$$\begin{aligned} &a_{11}^{(u)} \simeq 1.893\,91 + 0.404\,032i, \qquad a_{12}^{(u)} = a_{21}^{(u)} \simeq -1.429\,26 - 0.008\,986\,59i, \\ &a_{13}^{(u)} = a_{31}^{(u)} \simeq 0.704\,581 + 0.284\,696i, \qquad a_{22}^{(u)} \simeq 1.348\,23 - 0.002\,032\,71i, \\ &a_{23}^{(u)} = a_{32}^{(u)} \simeq -0.070\,3718 + 0.014\,833\,8i\,, \quad a_{33}^{(u)} \simeq 0.989\,285 - 0.000\,056\,837i, \\ &a_{11}^{(d)} \simeq 0.564\,554, \\ &a_{22}^{(d)} \simeq -0.534\,463, \qquad a_{23}^{(d)} = a_{32}^{(d)} \simeq 1.080\,71, \qquad a_{33}^{(d)} \simeq 1.421\,19 \end{aligned} \tag{3}$$

are $\mathcal{O}(1)$ dimensionless couplings. The values of the $\mathcal{O}(1)$ dimensionless couplings given above allows one to successfully reproduce the experimental values of the quark mass spectrum, CKM parameters, and Jarlskog invariant. As indicated by Table 2, our model is consistent with the low-energy quark flavor data. Note that we use the M_Z-scale experimental values of the quark masses given by Ref. [30] (which are similar to those in Ref. [31]). The experimental values of the CKM parameters are taken from Ref. [32].

With the aim of studying the sensitivity of the obtained values for the SM quark masses under variations around the best-fit values (maximum variation around 20% of their best-fit values), we show in Figs. 1 and 2 the correlations between the first- and second- as well as between the third- and second-generation SM quark masses. We have found that such variations yield values for the SM quark masses inside the 3σ experimentally allowed range, with the exception of the top and bottom quark masses where the majority of points are outside the 3σ range. Consequently the quark sector model parameters feature some moderate amount of fine tuning. We have numerically checked that the up- and down-type quark sector parameters have to be varied in range around 3% and 4% of their best-fit values, respectively, in order to obtain all SM quark masses inside the 3σ experimentally allowed range.

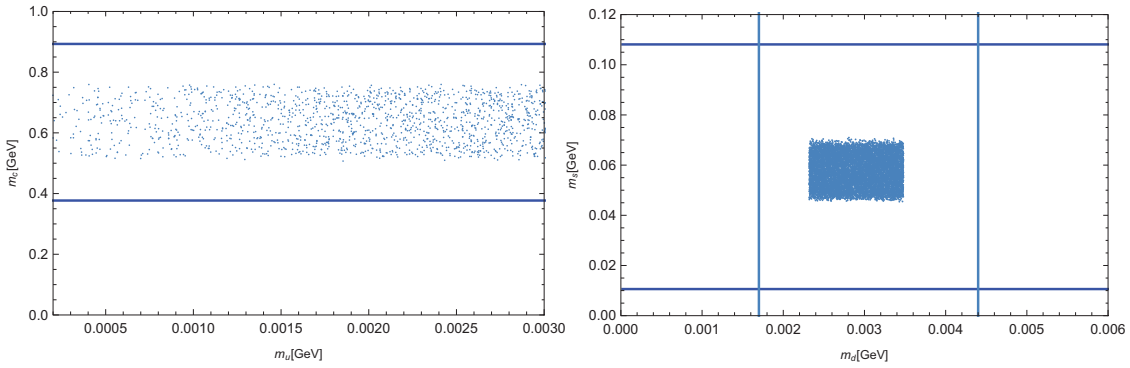

Fig. 1. Correlations between the first- and second-generation SM quark masses. The horizontal and vertical lines are the minimum and maximum values of the second- and first-generation quark masses, respectively, inside the 3σ experimentally allowed range.

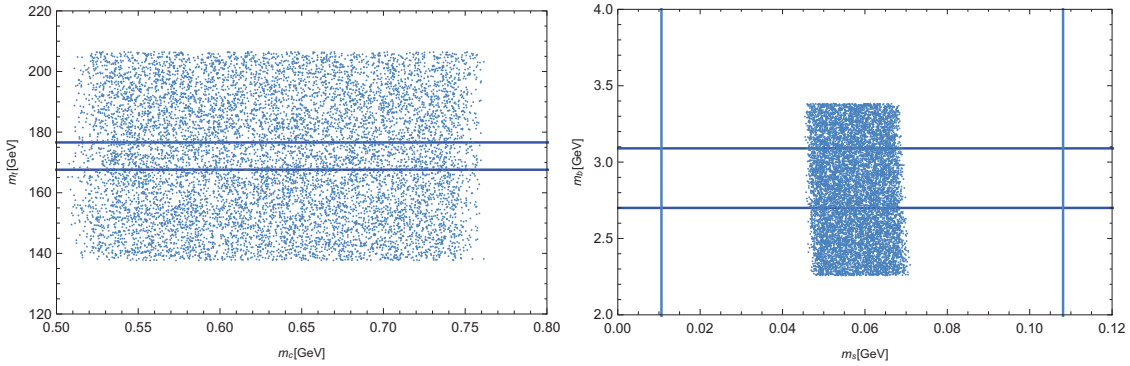

Fig. 2. Correlations between the second- and third-generation SM quark masses. The horizontal and vertical lines are the minimum and maximum values of the third- and second-generation quark masses, respectively, inside the 3σ experimentally allowed range.

Table 3. $SU(2)_L \times U(1)_L \times S_4 \times Z_2 \times Z_3 \times Z_4$ assignments for leptons and scalars.

	ψ_L	l_{1R}	$l_{2,3R}$	ν_R	N_L	N_R	S_L	S_R	ϕ	φ	ξ	ρ
$SU(2)_L$	2	1	1	1	1	1	1	1	1	1	1	1
$U(1)_L$	1	1	1	1	1	1	1	1	0	0	0	0
S_4	$\underline{3}$	$\underline{1}$	$\underline{2}$	$\underline{3}$	$\underline{3}$	$\underline{3}$	$\underline{3}$	$\underline{3}$	$\underline{3}$	$\underline{3}$	$\underline{1}$	$\underline{1}$
Z_2	1	1	1	1	1	-1	1	-1	-1	-1	-1	-1
Z_3	1	1	1	ω	ω^2	1	ω^2	1	1	ω	ω	1
Z_4	i	i	i	1	$-i$	i	$-i$	i	1	-1	-1	i

4. Lepton masses and mixings

The lepton fields and the corresponding scalars in lepton sectors, under $[SU(2)_L, U(1)_L, S_4, Z_2, Z_3, Z_4]$, is given in Table 3. The lepton Yukawa terms invariant under the symmetries of the model are:

$$\begin{aligned}
-\mathcal{L}_l = {} & \frac{h_1}{\Lambda}(\bar{\psi}_L\phi)_{\underline{1}}Hl_{1R} + \frac{h_2}{\Lambda}(\bar{\psi}_L\phi)_{\underline{2}}(Hl_R)_{\underline{2}} + \frac{h_3}{\Lambda}(\bar{\psi}_L\phi)_{\underline{2}}(H'l_R)_{\underline{2}} \\
& + x_1(\bar{\psi}_L N_R)_1\widetilde{H} + x_2(\bar{\psi}_L S_R)_1\widetilde{H} + \frac{y_1}{\Lambda}(\overline{N}_L\nu_R)_1\xi\rho + \frac{y_2}{\Lambda}(\overline{S}_L\nu_R)_1\xi\rho \\
& + z_1(\overline{S}_L N_R)_1\xi^\dagger + z_2(\overline{S}_L N_R)_{3_s}\varphi^\dagger + t_1(\overline{N}_L S_R)_1\xi^\dagger + t_2(\overline{N}_L S_R)_{3_s}\varphi^\dagger \\
& + w_1(\overline{N}_L N_R)_1\xi^\dagger + w_2(\overline{N}_L N_R)_{3_s}\varphi^\dagger + w_3(\overline{S}_L S_R)_1\xi^\dagger + w_4(\overline{S}_L S_R)_{3_s}\varphi^\dagger + \text{H.c.} \qquad (4)
\end{aligned}$$

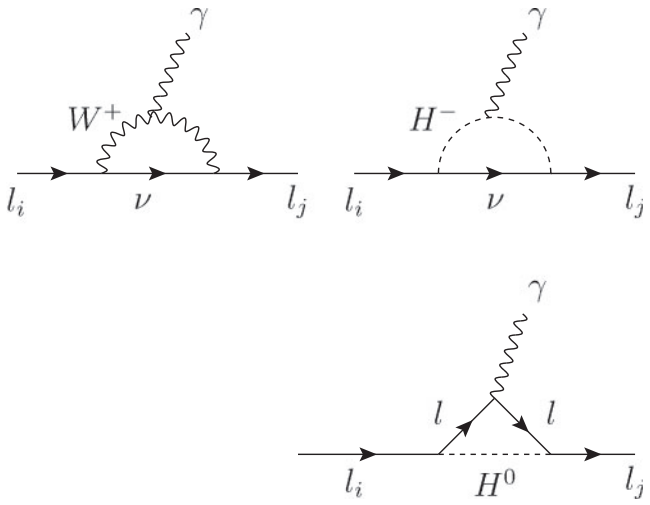

Fig. 3. Feynman diagrams contributing to lepton flavor changing decay. Here $i \neq j$, $i = \tau, \mu$, and $j = \mu, e$.

In the case where S_4 is spontaneously broken down to {identity} by the VEV alignment $\langle \phi_1 \rangle = v$, $\langle \phi_2 \rangle = ve^{i\alpha}$, $\langle \phi_3 \rangle = ve^{i\beta}$ and $\langle H \rangle = v_h$, $\langle H' \rangle = v'_h$ within the following expansions

$$\phi_i = \langle \phi_i \rangle + \phi'_i \ (i = 1, 2, 3), \tag{5}$$

we get the lepton flavor changing interactions as follows:

$$\begin{aligned} -\mathcal{L}^{\text{clep}} \subset & \frac{h_1 v}{\Lambda}(\bar{\nu}_{1L}H^+ + \bar{l}_{1L}H^0)l_{1R} + \frac{h_2 v}{\Lambda}(\bar{\nu}_{1L}H^+ + \bar{l}_{1L}H^0)l_{2R} \\ & + \frac{h_3 v}{\Lambda}(\bar{\nu}_{1L}H'^+ + \bar{l}_{1L}H'^0)\bar{l}_{2R} + \frac{h_2 v}{\Lambda}(\bar{\nu}_{1L}H^+ + \bar{l}_{1L}H^0)\bar{l}_{3R} \\ & - \frac{h_3 v}{\Lambda}(\bar{\nu}_{1L}H'^+ + \bar{l}_{1L}H'^0)l_{3R} + \frac{h_1 v}{\Lambda}(\bar{\nu}_{2L}H^+ + \bar{l}_{2L}H^0)l_{1R} + \text{H.c.} \end{aligned} \tag{6}$$

From Eq. (6), it follows that, in the model under consideration, the usual Yukawa couplings are associated with the factor $\frac{v}{\Lambda}$ and the lepton flavor changing decays consist of the contribution of three Feynman diagrams as in Fig. 3. The current experimental data on lepton flavor changing decays read [32]: $\text{Br}(\mu^- \to e^-\gamma) < 4.2 \times 10^{-13}$, $\text{Br}(\tau^- \to e^-\gamma) < 3.3 \times 10^{-8}$, and $\text{Br}(\tau^- \to \mu^-\gamma) < 4.4 \times 10^{-8}$. The partial decay width is given by [36,37]

$$\Gamma(l_i \to l_j\gamma) = \frac{(m_i^2 - m_j^2)^3}{16\pi m_i^3}\left(|C_L|^2 + |C_R|^2\right), \tag{7}$$

where the above form factors C_L and C_R are determined from the process amplitude [36,37]

$$\begin{aligned} \mathcal{M} = & 2(p_i \cdot \epsilon)\left[C_L\bar{u}_j(p_j)P_L u_i(p_i) + C_R\bar{u}_j(p_j)P_R u_i(p_i)\right] \\ & - (m_i C_R + m_j C_L)\bar{u}_j(p_j)\not{\epsilon}P_L u_i(p_i) - (m_i C_L + m_j C_R)\bar{u}_j(p_j)\not{\epsilon}P_R u_i(p_j). \end{aligned} \tag{8}$$

For the case $m_i \gg m_j$, we get

$$\text{Br}(l_i \to l_j\gamma) = \frac{12\pi^2}{G_F^2}\left(|D_L|^2 + |D_R|^2\right)\text{Br}(l_i \to l_j\bar{\nu}_j\nu_i), \tag{9}$$

where $G_F = g^2/(4\sqrt{2}m_W^2)$. In the model under consideration, one has [37,38]

$$D_L \propto \frac{v}{M_H \Lambda}\mathcal{O}(m_j/m_i), \quad D_R \propto \frac{v}{M_H \Lambda} \tag{10}$$

where M_H is the mass scale of the heavy scalars (which provide the dominant contributions to the lepton flavor violation decays) running in the internal lines of the loop. For further details on the form factors $D_{L,R}$, the reader is referred to Refs. [36–39].

Combining Eqs. (9) and (10), we see that the lepton flavor changing processes in this model are suppressed by the factor $\frac{v}{\Lambda G_F^2 M_H^2}$ associated with the above-mentioned small Yukawa couplings and the large mass scale of the heavy scalars running in the internal lines of the loop.

Let us turn to the lepton mass issue. From Eq. (4), the lepton mass terms read

$$\begin{aligned}
-\mathcal{L}_{cl}^{\rm mass} &= \frac{v_1}{\Lambda}h_1 v_h \bar{l}_{1L} l_{1R} + \frac{v_1}{\Lambda}\left(h_2 v_h + h_3 v_h'\right)\bar{l}_{1L} l_{2R} + \frac{v_1}{\Lambda}\left(h_2 v_h - h_3 v_h'\right)\bar{l}_{1L} l_{3R} \\
&+ \frac{v_2}{\Lambda}h_1 v_h \bar{l}_{2L} l_{1R} + \frac{v_2}{\Lambda}\left(h_2 v_h + h_3 v_h'\right)\omega\bar{l}_{2L} l_{2R} + \frac{v_2}{\Lambda}\left(h_2 v_h - h_3 v_h'\right)\omega^2\bar{l}_{2L} l_{3R} \\
&+ \frac{v_3}{\Lambda}h_1 v_h \bar{l}_{3L} l_{1R} + \frac{v_3}{\Lambda}\left(h_2 v_h + h_3 v_h'\right)\omega^2\bar{l}_{3L} l_{2R} + \frac{v_3}{\Lambda}\left(h_2 v_h - h_3 v_h'\right)\omega\bar{l}_{3L} l_{3R} + \text{H.c.} \\
&\equiv (\bar{l}_{1L} \quad \bar{l}_{2L} \quad \bar{l}_{3L}) M_l (l_{1R} \quad l_{2R} \quad l_{3R})^T + \text{H.c.},
\end{aligned} \tag{11}$$

where the mass matrix for charged leptons is given by:

$$M_l = \frac{v}{\Lambda}\begin{pmatrix} h_1 v_h & h_2 v_h + h_3 v_h' & h_2 v_h - h_3 v_h' \\ h_1 v_h e^{i\alpha} & (h_2 v_h + h_3 v_h')e^{i\alpha}\omega^2 & (h_2 v_h - h_3 v_h')e^{i\alpha}\omega \\ h_1 v_h e^{i\beta} & (h_2 v_h + h_3 v_h')e^{i\beta}\omega & (h_2 v_h - h_3 v_h')e^{i\beta}\omega^2 \end{pmatrix}. \tag{12}$$

This matrix can be diagonalized as

$$U_L^\dagger M_l U_R = \frac{\sqrt{3}v}{\Lambda}\text{diag}(h_1 v_h,\, h_2 v_h - h_3 v_h',\, h_2 v_h + h_3 v_h') \equiv \text{diag}(m_e,\, m_\mu,\, m_\tau), \tag{13}$$

where

$$U_L = \frac{1}{\sqrt{3}}\begin{pmatrix} 1 & 0 & 0 \\ 0 & e^{i\alpha} & 0 \\ 0 & 0 & e^{i\beta} \end{pmatrix}\begin{pmatrix} 1 & 1 & 1 \\ 1 & \omega^2 & \omega \\ 1 & \omega & \omega^2 \end{pmatrix}, \quad U_R = 1, \tag{14}$$

$$m_e = \frac{\sqrt{3}v}{\Lambda}h_1 v_h, \quad m_{\mu,\tau} = \frac{\sqrt{3}v}{\Lambda}\left(h_2 v_h \pm h_3 v_h'\right), \tag{15}$$

where $\omega = e^{i2\pi/3}$ is the cube root of unity.

The best-fit values for the masses of charged leptons are given in Ref. [2]: $m_e \simeq 0.510\,99$ MeV, $m_\mu \simeq 105.658\,37$ MeV, $m_\tau \simeq 1776.86$ MeV. Then, we find the relations $\frac{h_3}{h_2} \simeq \frac{v_h}{v_h'}$, $\frac{h_2}{h_1} \simeq 10^3$.

We also assume that in the neutrino sector, the S_4 discrete group is spontaneously broken down to the Klein four group $\mathcal{K}$ by the VEV alignment $\langle\varphi\rangle = (0, v_\varphi, 0)$ of φ and the VEVs of ξ, ρ as $\langle\xi\rangle = v_\xi$, $\langle\rho\rangle = v_\rho$. In this case, the neutrino mass matrices become

$$m_{\nu N} = x_1 v_h \mathbf{I} \equiv a_1 \mathbf{I}, \quad M_{\nu S} = x_2 v_h \mathbf{I} \equiv a_2 \mathbf{I}, \tag{16}$$

$$m'_{\nu N} = \frac{y_1 v_\xi v_\rho}{\Lambda}\mathbf{I} \equiv b_1 \mathbf{I}, \; M'_{\nu S} = \frac{y_2 v_\xi v_\rho}{\Lambda}\mathbf{I} \equiv b_2 \mathbf{I}, \tag{17}$$

$$M'_{NS} = \begin{pmatrix} z_1 v_\xi & 0 & z_2 v_\varphi \\ 0 & z_1 v_\xi & 0 \\ z_2 v_\varphi & 0 & z_1 v_\xi \end{pmatrix} \equiv \begin{pmatrix} c_1 & 0 & c_2 \\ 0 & c_1 & 0 \\ c_2 & 0 & c_1 \end{pmatrix}, \tag{18}$$

$$M_{NS} = \begin{pmatrix} t_1 v_\xi & 0 & t_2 v_\varphi \\ 0 & t_1 v_\xi & 0 \\ t_2 v_\varphi & 0 & t_1 v_\xi \end{pmatrix} \equiv \begin{pmatrix} d_1 & 0 & d_2 \\ 0 & d_1 & 0 \\ d_2 & 0 & d_1 \end{pmatrix}, \tag{19}$$

$$M_{NN} = \begin{pmatrix} w_1 v_\xi & 0 & w_2 v_\varphi \\ 0 & w_1 v_\xi & 0 \\ w_2 v_\varphi & 0 & w_1 v_\xi \end{pmatrix} \equiv \begin{pmatrix} g_1 & 0 & g_2 \\ 0 & g_1 & 0 \\ g_2 & 0 & g_1 \end{pmatrix}, \tag{20}$$

$$M_{SS} = \begin{pmatrix} w_3 v_\xi & 0 & w_4 v_\varphi \\ 0 & w_3 v_\xi & 0 \\ w_4 v_\varphi & 0 & w_3 v_\xi \end{pmatrix} \equiv \begin{pmatrix} g_3 & 0 & g_4 \\ 0 & g_3 & 0 \\ g_4 & 0 & g_3 \end{pmatrix}. \tag{21}$$

Let us note that the matrices given by Eqs. (16)–(21) are all symmetric and $m_{\nu N}$, $M_{\nu S}$, M'_{NS}, M_{NS}, M_{NN}, M_{SS} are respectively generated from the renormalizable Yukawa interactions $x_1(\bar{\psi}_L N_R)_1 \widetilde{H}$, $x_2(\bar{\psi}_L S_R)_1 \widetilde{H}$, $\{z_1(\overline{S}_L N_R)_1 \xi^\dagger, z_2(\overline{S}_L N_R)_{3_s} \varphi^\dagger\}$, $\{t_1(\overline{N}_L S_R)_1 \xi^\dagger, t_2(\overline{N}_L S_R)_{3_s} \varphi^\dagger\}$, $\{w_1(\overline{N}_L N_R)_1 \xi^\dagger, w_2(\overline{N}_L N_R)_{3_s} \varphi^\dagger\}$, $\{w_3(\overline{S}_L S_R)_1 \xi^\dagger, w_4(\overline{S}_L S_R)_{3_s} \varphi^\dagger\}$, whereas $m'_{\nu N}$ and $M'_{\nu S}$ arise from the non-renormalizable Yukawa interactions $\frac{y_1}{\Lambda}(\overline{N}_L \nu_R)_1 \xi \rho$ and $\frac{y_2}{\Lambda}(\overline{S}_L \nu_R)_1 \xi \rho$, respectively.

In this work, we introduce the $Z_2 \times Z_3 \times Z_4 \times Z_{14} \times U(1)_L$ symmetry[1], which in addition to the S_4 symmetry prevents some Yukawa interactions thus giving rise to the predictive textures for the neutrino sector shown in Eqs. (16)–(21). For instance, since the product of two S_4 triplets contains an S_4 triplet, the coupling $\overline{\psi}_L N_R$ can transform under $S_4 \times Z_2 \times Z_3 \times Z_4 \times Z_{14} \times U(1)_L$ as $\sim (\underline{3} \otimes \underline{3}, -1, 1, 1, 1, 0)$, which implies that in order to generate the mass matrix $m_{\nu N}$, one needs one S_4 singlet transforming as $(\underline{1}, -1, 1, 1, 1, 0)$, in order to build an invariant under all given symmetries. For the known scalars, $(\overline{\psi}_L N_R)\widetilde{H}'$ is forbidden by the S_4 symmetry, $(\overline{\psi}_L N_R)\widetilde{H}''$ is prevented by the Z_2 symmetry, $(\overline{\psi}_L N_R)\chi$ is not allowed by the Z_2, Z_{14} and $SU(2)_L$ symmetries, whereas $(\overline{\psi}_L N_R)\xi$ is forbidden by the Z_3 and Z_4 symmetries and $(\overline{\psi}_L N_R)\rho$ is prevented by the Z_4 symmetry. Consequently, there is only one term involving the fields ψ_L, N_R, and H, invariant under the $S_4 \times Z_2 \times Z_3 \times Z_4 \times Z_{14} \times U(1)_L$ symmetry, which corresponds to $x_1(\bar{\psi}_L N_R)_1 \widetilde{H}$ as in Eq. (4) that provide a simple form of $m_{\nu N}$ as indicated by Eq. (16). The situation is similar for the remaining couplings that generate the other mass matrices given in Eqs. (16)–(21).

In the basis (ν, N, S), the full neutrino mass matrix predicted by our model takes the form:

$$M_{\rm eff} = \begin{pmatrix} 0 & m_{\nu N} & M_{\nu S} \\ m'_{\nu N} & M_{NN} & M_{NS} \\ M'_{\nu S} & M'_{NS} & M_{SS} \end{pmatrix}. \tag{22}$$

The light active neutrino masses are obtained by diagonalizing the matrix given by Eq. (22) and this is done by introducing the following matrices:

$$M_D = (m_{\nu N} \;\; M_{\nu S}),\; M_D^T = \begin{pmatrix} m'_{\nu N} \\ M'_{\nu S} \end{pmatrix},\; M_R = \begin{pmatrix} M_{NN} & M_{NS} \\ M'_{NS} & M_{SS} \end{pmatrix}.$$

[1] All the lepton fields and the corresponding scalars in Table 3 carry the same charge (+ 1) under Z_{14}, which is not necessary to write out here.

The effective neutrino mass matrix $M_{\rm eff}$ in Eq. (22) can be rewritten in the form:

$$M_{\rm eff} = \begin{pmatrix} 0 & M_D \\ M_D^T & M_R \end{pmatrix}, \tag{23}$$

which is similar to the one resulting from a type-I seesaw mechanism. Then, the light active neutrino mass matrix takes the form:

$$\begin{aligned} m_\nu &= -M_D M_R^{-1} M_D^T = -m_{\nu N} M'^{-1}_{NS} M'_{\nu S} - M_{\nu S} M^{-1}_{NS} m'_{\nu N} \\ &- M_{\nu S} M^{-1}_{SS} M'_{\nu S} + m_{\nu N} M^{-1}_{NN} M_{NS} M^{-1}_{SS} M'_{\nu S} + M_{\nu S} M^{-1}_{SS} M'_{NS} M^{-1}_{NN} m'_{\nu N} \\ &+ M_{\nu S} M^{-1}_{NS} M_{NN} M'^{-1}_{NS} M'_{\nu S} - m_{\nu N} M^{-1}_{NN} M_{NS} M^{-1}_{SS} M'_{NS} M^{-1}_{NN} m'_{\nu N}. \end{aligned} \tag{24}$$

Replacing Eqs. (16)–(21) in Eq. (24) yields the following mass matrix for light active neutrinos:

$$m_\nu = \begin{pmatrix} A & 0 & B \\ 0 & C & 0 \\ B & 0 & A \end{pmatrix}, \tag{25}$$

where

$$\begin{aligned} A &= \frac{1}{2}\left(a_1\alpha_1 + a_2\alpha_2\right), \; B = \frac{1}{2}\left(a_1\beta_1 + a_2\beta_2\right), \\ C &= \frac{a_2 b_2 g_1 - a_2 b_1 c_1 - a_1 b_2 d_1}{c_1 d_1} - \frac{(a_1 d_1 - a_2 g_1)(b_1 c_1 - b_2 g_1)}{g_1^2 g_3}, \end{aligned} \tag{26}$$

$$\begin{aligned} \alpha_1 &= -\frac{2b_2 c_1}{c_1^2 - c_2^2} + \frac{(d_1 - d_2)[b_2(g_1 - g_2) - b_1(c_1 - c_2)]}{(g_1 - g_2)^2(g_3 - g_4)} + \frac{(d_1 + d_2)[b_2(g_1 + g_2) - b_1(c_1 + c_2)]}{(g_1 + g_2)^2(g_3 + g_4)}, \\ \alpha_2 &= -\frac{2b_1 d_1}{d_1^2 - d_2^2} - \frac{2b_2[(c_1 d_1 + c_2 d_2)g_1 - (c_2 d_1 + c_1 d_2)g_2]}{(c_1^2 - c_2^2)(d_1^2 - d_2^2)} + \frac{b_1(c_1 - c_2)}{(g_1 - g_2)(g_3 - g_4)} \\ &+ \frac{b_1(c_1 + c_2)}{(g_1 + g_2)(g_3 + g_4)} - \frac{2b_2 g_3}{g_3^2 - g_4^2}, \\ \beta_1 &= \frac{2b_2 c_2}{c_1^2 - c_2^2} + \frac{(d_1 - d_2)[b_1(c_1 - c_2) - b_2(g_1 - g_2)]}{(g_1 - g_2)^2(g_3 - g_4)} + \frac{(d_1 + d_2)[b_2(g_1 + g_2) - b_1(c_1 + c_2)]}{(g_1 + g_2)^2(g_3 + g_4)}, \\ \beta_2 &= \frac{2b_1 d_2}{d_1^2 - d_2^2} + \frac{2b_2[(c_1 d_1 + c_2 d_2)g_2 - (c_2 d_1 + c_1 d_2)g_1]}{(c_1^2 - c_2^2)(d_1^2 - d_2^2)} - \frac{b_1(c_1 - c_2)}{(g_1 - g_2)(g_3 - g_4)} \\ &+ \frac{b_1(c_1 + c_2)}{(g_1 + g_2)(g_3 + g_4)} + \frac{2b_2 g_4}{g_3^2 - g_4^2}, \end{aligned} \tag{27}$$

with $a_{1,2}$, $b_{1,2}$, $c_{1,2}$, $d_{1,2}$, and $g_{1,2,3,4}$ defined in Eqs. (16)–(21). The mass matrix m_ν for light active neutrinos is diagonalized by the rotation matrix U_ν,

$$U_\nu = \begin{pmatrix} \frac{1}{\sqrt{2}} & 0 & -\frac{1}{\sqrt{2}} \\ 0 & 1 & 0 \\ \frac{1}{\sqrt{2}} & 0 & \frac{1}{\sqrt{2}} \end{pmatrix}, \tag{28}$$

and the light active neutrino masses $m_{1,2,3}$ are given by

$$m_1 = A + B, \quad m_2 = C, \quad m_3 = A - B. \tag{29}$$

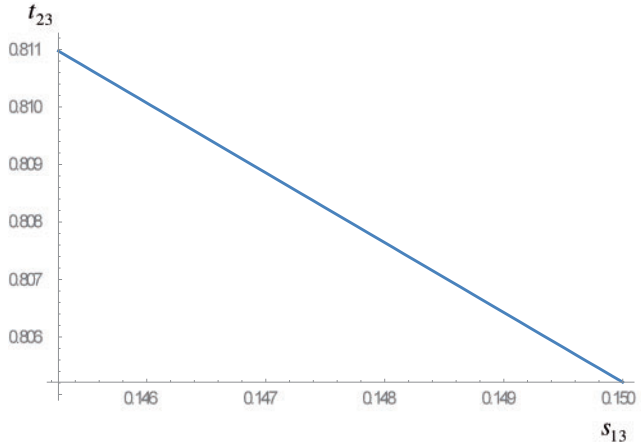

Fig. 4. t_{23} as a function of s_{13} with $s_{13} \in (\sqrt{0.0211}, \sqrt{0.0225})$ rad.

By combining Eqs. (14) and (28) we find that the leptonic mixing matrix takes the form:

$$U^{\rm lep} = U_L^\dagger U_\nu = \begin{pmatrix} \frac{1+e^{-i\beta}}{\sqrt{6}} & \frac{e^{-i\alpha}}{\sqrt{3}} & \frac{-1+e^{-i\beta}}{\sqrt{6}} \\ \frac{1+\omega^2 e^{-i\beta}}{\sqrt{6}} & \frac{\omega e^{-i\alpha}}{\sqrt{3}} & \frac{-1+\omega^2 e^{-i\beta}}{\sqrt{6}} \\ \frac{1+\omega e^{-i\beta}}{\sqrt{6}} & \frac{\omega^2 e^{-i\alpha}}{\sqrt{3}} & \frac{-1+\omega e^{-i\beta}}{\sqrt{6}} \end{pmatrix}. \tag{30}$$

We see that all the elements of the matrix $U^{\rm lep}$ in Eq. (30) depend only on two parameters α and β. From experimental constraints on the elements of the lepton mixing matrix given in Ref. [33], we can find out the regions of α and β to establish experimental constraints for the lepton mixing matrix. In the standard Particle Data Group (PDG) parametrization, the leptonic mixing matrix can be parametrized in three Euler's angles as follows:

$$s_{13} = |U_{13}| = \frac{\sqrt{1-\cos\beta}}{\sqrt{3}}, \tag{31}$$

$$t_{23} = \left|\frac{U_{23}}{U_{33}}\right| = \left|\frac{1+2\cos\beta}{2+\cos\beta-\sqrt{3}\sin\beta}\right|, \tag{32}$$

$$t_{12} = \left|\frac{U_{12}}{U_{11}}\right| = \sqrt{\frac{1}{1+\cos\beta}}, \tag{33}$$

i.e., s_{13}, t_{12}, and t_{23} in Eqs. (31) and (33) depend only on one parameter β. Equations (31)–(33) yield:

$$\beta = -\arccos(1-3s_{13}^2), \tag{34}$$

$$t_{23} = \frac{1-2s_{13}^2}{1-s_{13}^2+s_{13}\sqrt{2-3s_{13}^2}},$$

$$t_{12} = \frac{1}{\sqrt{2-3s_{13}^2}}. \tag{35}$$

The data from the Particle Data Group from 2018 [2] shows that $s_{13} \in (0.145\,258, 0.15)$ rad so $t_{23} \in (0.806, 0.811)$ and $t_{12} \in (0.7811, 0.7192)$ rad as depicted in Figs. 4 and 5, respectively. Taking

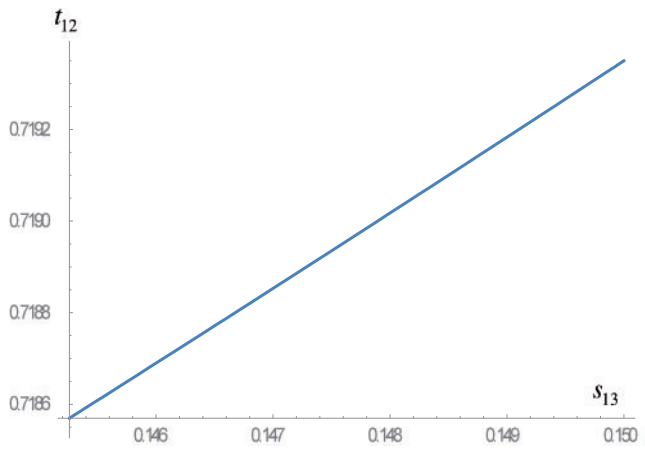

Fig. 5. t_{12} as a function of s_{13} with $s_{13} \in (\sqrt{0.0211}, \sqrt{0.0225})$ rad.

the best-fit value given in Ref. [2], $s_{13} = 0.147\,648$ rad ($\theta_{13} = 8.459\,63°$) we get $t_{23} = 0.808\,068$ ($\theta_{23} = 38.9406°$) and $t_{12} = 0.718\,959$ ($\theta_{12} = 35.7146°$), which are in good agreement with the values of θ_{23} and θ_{12} given in Ref. [2]. On the other hand, with this best value of θ_{13}, we get $\beta = -0.363\,663$ rad ($\sim 339.163°$) and Dirac CP-violating phase $\delta_{\rm CP} = 259.579°$, which is a viable value of the CP-violating Dirac phase [2]. The leptonic mixing matrix in Eq. (36) takes the explicit form

$$U^{\rm lep} = \begin{pmatrix} 0.789\,797 + 0.145\,214i & 0.577\,35e^{-ia} & -0.026\,6994 + 0.145\,214i \\ 0.343\,233 - 0.403\,038i & (-0.288\,675 + 0.5i)e^{-ia} & -0.473\,264 - 0.403\,038i \\ 0.091\,7147 + 0.257\,824i & (-0.288\,675 - 0.5i)e^{-ia} & -0.724\,782 + 0.257\,824i \end{pmatrix}, \tag{36}$$

which is a unitary matrix.

The expression (36) shows that α is free parameter so we can choose the VEV alignment ϕ in the charged-lepton sector as $\langle\phi\rangle = v(1, 1, e^{i\beta})$, i.e., α may get the value $\alpha = 0$. In this case, the leptonic mixing matrix becomes:

$$U^{\rm lep} = \begin{pmatrix} 0.789\,797 + 0.145\,214i & 0.577\,35 & -0.026\,6994 + 0.145\,214i \\ 0.343\,233 - 0.403\,038i & -0.288\,675 + 0.5i & -0.473\,264 - 0.403\,038i \\ 0.091\,7147 + 0.257\,824i & -0.288\,675 - 0.5i & -0.724\,782 + 0.257\,824i \end{pmatrix}, \tag{37}$$

or

$$|U^{\rm lep}| = \begin{pmatrix} 0.803\,036 & 0.577\,35 & 0.147\,648 \\ 0.529\,385 & 0.577\,35 & 0.621\,625 \\ 0.273\,651 & 0.577\,35 & 0.769\,274 \end{pmatrix}, \tag{38}$$

i.e., the ranges of the magnitudes of the elements of the three-flavor leptonic mixing matrix are consistent with those of given in Ref. [33]. At present, the values of neutrino masses (or the absolute neutrino masses) as well as the mass ordering of neutrinos are still unknown. The result in Ref. [34] shows that $m_i \leq 0.6$ eV ($i = 1, 2, 3$) while the upper bound on the sum of light active neutrino

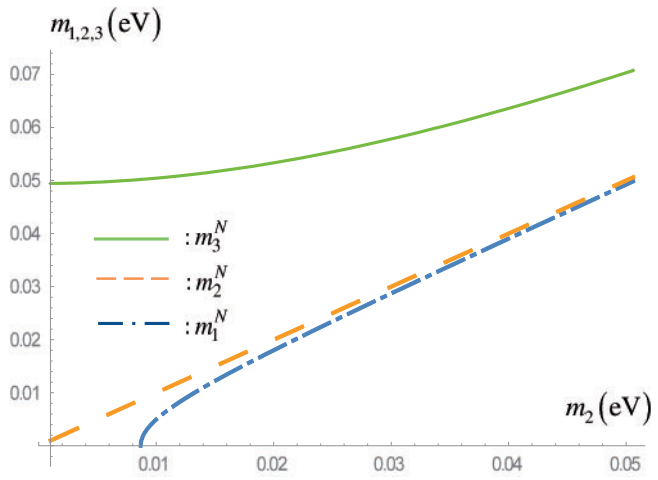

Fig. 6. $m_{1,3}$ as functions of m_2 with $m_2 \in (0.001, 0.0506)$ in the normal spectrum.

masses is given by [35]

$$\sum_{i=1}^{3} m_i \leq 0.17\,\text{eV}. \tag{39}$$

The experimental neutrino oscillation data given in Eq. (1) are compatible with two possible signs of Δm^2_{23}, which is currently unknown, and correspond to two types of neutrino mass spectra.

4.1. Normal spectrum ($m_1 < m_2 < m_3$)

By taking the best-fit values on neutrino mass squared differences for the normal spectrum, given in Ref. [2], $\Delta m^2_{21} = 7.53 \times 10^{-5}\text{eV}^2$ and $\Delta m^2_{32} = 2.444 \times 10^{-3}\text{eV}^2$, we obtain four solutions; however, they have the same absolute values of $m_{1,2,3}$; the unique difference is the sign of them. So, here we only consider the following solution:

$$\begin{aligned} A &= 1.581\,14 \times 10^{-2}\Gamma, \\ B &= \left(-0.014\,8662 - 12.5522C^2 + 7.938\,71 \times 10^{-3}\gamma\right)\Gamma, \end{aligned} \tag{40}$$

where

$$\begin{aligned} \Gamma &= \sqrt{2.3687 + 2 \times 10^3 C^2 + 1.264\,91\sqrt{\gamma}}, \\ \gamma &= \sqrt{-0.460\,083 + 5.921\,75 \times 10^3 C^2 + 2.5 \times 10^6 C^4}. \end{aligned} \tag{41}$$

In the model under consideration, $C \equiv m_2 \in (0.001, 0.0506)\,\text{eV}$ is a good region of C that can reach the realistic normal neutrino mass hierarchy that is depicted in Fig. 7. In the case $C \equiv m_2 = 0.0087\,\text{eV}$, the parameters A, B and the other neutrino masses are explicitly given as $A = 2.541\,05 \times 10^{-2}, B = -2.4786 \times 10^{-2}$, $m_1 = 6.245 \times 10^{-4}\,\text{eV}$, and $m_3 = 5.019\,65 \times 10^{-2}\,\text{eV}$, which corresponds to a normal neutrino mass spectrum. The sum of all three neutrinos in this case is given by $\sum^N = \sum_{i=1}^3 m_i = 5.9521 \times 10^{-2}\text{eV}$ lying within the cosmological bound from the Planck data given in Eq. (39).

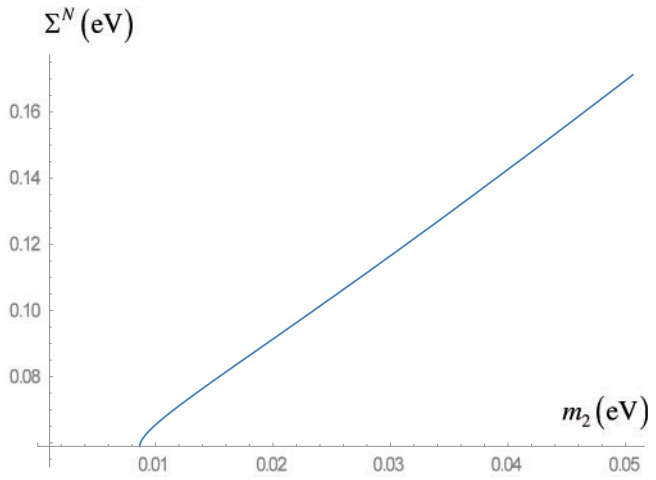

Fig. 7. $\sum^N = \sum_{i=1}^3 m_i^N$ as functions of m_2 with $m_2 \in (0.001, 0.0506)$ in the normal spectrum.

4.2. Inverted spectrum ($m_3 < m_1 < m_2$)

Similar to the normal spectrum, by taking the best-fit values on neutrino mass squared differences for the inverted spectrum, given in Ref. [2], $\Delta m_{21}^2 = 7.53 \times 10^{-5}\text{eV}^2$ and $\Delta m_{32}^2 = -2.53 \times 10^{-3}\text{eV}^2$, we get a solution as follows:

$$\begin{aligned} A &= 1.5811 \times 10^{-2}\Gamma', \\ B &= \left(-0.016\,7814 + 12.8825C^2 - 1.2882 \times 10^{-2}\gamma'\right)\Gamma', \end{aligned} \tag{42}$$

where

$$\begin{aligned} \Gamma' &= \sqrt{2.6053 + 2 \times 10^3 C^2 + 2\sqrt{\gamma'}}, \\ \gamma' &= \sqrt{0.190\,509 - 2.6053 \times 10^3 C^2 + \times 10^6 C^4}. \end{aligned} \tag{43}$$

In this model, $C \equiv m_2 \in (0.051, 0.065)$ eV is a good region of C that can reach the inverted neutrino mass hierarchy that is depicted in Fig. 8. In the case $C \equiv m_2 = 5.1 \times 10^{-2}$ eV, the parameters A, B and the other neutrino masses are explicitly given as $A = 2.934\,12 \times 10^{-2}, B = 2.091\,51 \times 10^{-2}$, $m_1^I = 5.025\,63 \times 10^{-2}$ eV, and $m_3^I = 8.426\,15 \times 10^{-3}$ eV, which corresponds to an inverted neutrino mass spectrum. The sum of all three neutrinos in this case is given by $\sum^I = \sum_{i=1}^3 m_i^I = 0.109\,68$ eV, which is consistent with the cosmological bound from the Planck data in Eq. (39).

5. Conclusions

We have proposed a low-scale seesaw model to generate the masses for the active neutrinos based on S_4 flavor symmetry supplemented by the $Z_2 \times Z_3 \times Z_4 \times Z_{14} \times U(1)_L$ group, where the masses of the SM charged fermions and the fermionic mixing angles are generated from a Froggatt–Nielsen mechanism after spontaneous breaking of the $S_4 \times Z_2 \times Z_3 \times Z_4 \times Z_{14} \times U(1)_L$ group. The obtained values for the physical observables of the quark and lepton sectors are in good agreement with the most recent experimental data. The Dirac CP-violating phase δ_{CP} is predicted to be 259.579°, which is consistent with the most recent neutrino oscillation experimental data [2]. The predictions for the absolute neutrino masses in the model can also saturate the recent constraints.

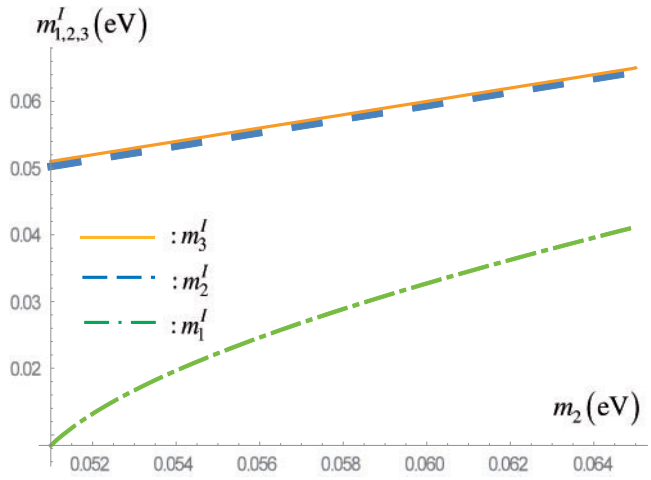

Fig. 8. $m^I_{1,3}$ as functions of $C \equiv m_2$ with $m_2 \in (0.051, 0.065)$ in the inverted spectrum.

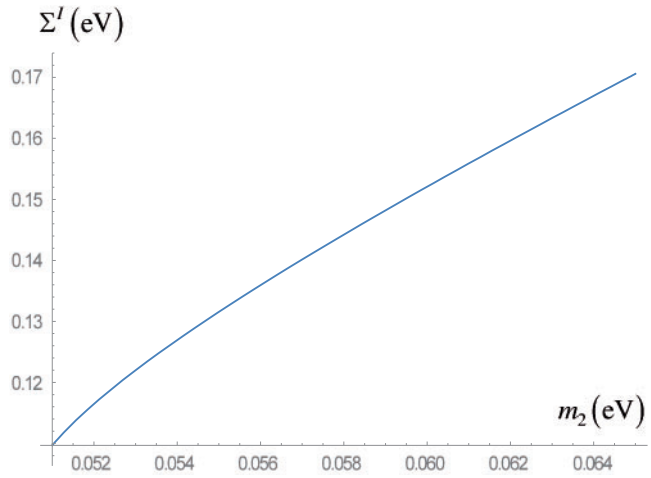

Fig. 9. $\sum^I = \sum_{i=1}^3 m^I_i$ as functions of m_2 with $m_2 \in (0.051, 0.065)$ in the inverted spectrum.

Acknowledgements

This research is funded by the Vietnam National Foundation for Science and Technology Development (NAFOSTED) under grant number 103.01-2017.341 as well as by Fondecyt (Chile), Grants No. 1170803, CONICYT PIA/Basal FB0821. H.N.L. acknowledges the warm hospitality at BLTP, JINR, and the financial support of the Vietnam Academy of Science and Technology under grant NVCC05.01/19-19. A.E.C.H. is very grateful to the Institute of Physics, Vietnam Academy of Science and Technology for the warm hospitality.

Funding

Open Access funding: SCOAP[3].

References

[1] A. E. Cárcamo Hernández, S. Kovalenko, H. N. Long, and I. Schmidt, J. High Energy Phys. **1807**, 144 (2018) [arXiv:1705.09169 [hep-ph]] [Search INSPIRE].
[2] M. Tanabashi et al. [Particle Data Group], Phys. Rev. D **98**, 030001 (2018) and 2019 update.
[3] N. Cabibbo, Phys. Rev. Lett. **10**, 531 (1963).
[4] M. Kobayashi and T. Maskawa, Prog. Theor. Phys. **49**, 652 (1973).
[5] Y. Cai, T. Han, T. Li, and R. Ruiz, Front. Phys. **6**, 40 (2018).

[6] R. N. Mohapatra, Phys. Rev. Lett. **56**, 561 (1986).
[7] R. N. Mohapatra and J. W. F. Valle, Phys. Rev. D **34**, 1642 (1986).
[8] M. Malinský, J. C. Romão, and J. W. F. Valle, Phys. Rev. Lett. **95**, 161801 (2005) [arXiv:hep-ph/0506296] [Search INSPIRE].
[9] P. S. Bhupal Dev and R. N. Mohapatra, Phys. Rev. D **81**, 013001 (2010) [arXiv:0910.3924 [hep-ph]] [Search INSPIRE].
[10] S. S. C. Law and K. L. McDonald, Phys. Rev. D **87**, 113003 (2013) [arXiv:1303.4887 [hep-ph]] [Search INSPIRE].
[11] B. Adhikary, A. Ghosal, and P. Roy, Indian J. Phys. **88**, 979 (2014) [arXiv:1311.6746 [hep-ph]] [Search INSPIRE].
[12] S. Fraser, E. Ma, and O. Popov, Phys. Lett. B **737**, 280 (2014) [arXiv:1408.4785 [hep-ph]] [Search INSPIRE].
[13] A. E. Cárcamo Hernández and I. de Medeiros Varzielas, J. Phys. G: Nucl. Part. Phys. **42**, 065002 (2015) [arXiv:1410.2481 [hep-ph]] [Search INSPIRE].
[14] A. Abada and M. Lucente, Nucl. Phys. B **885**, 651 (2014) [arXiv:1401.1507 [hep-ph]] [Search INSPIRE].
[15] A. Ghosal and R. Samanta, J. High Energy Phys. **1505**, 077 (2015) [arXiv:1501.00916 [hep-ph]] [Search INSPIRE].
[16] A. E. Cárcamo Hernández and R. Martinez, Nucl. Phys. B **905**, 337 (2016) [arXiv:1501.05937 [hep-ph]] [Search INSPIRE].
[17] A. E. Cárcamo Hernández, R. Martinez, and F. Ochoa, Eur. Phys. J. C **76**, 634 (2016) [arXiv:1309.6567 [hep-ph]] [Search INSPIRE].
[18] R. Sinha, R. Samanta, and A. Ghosal, Phys. Lett. B **759**, 206 (2016) [arXiv:1508.05227 [hep-ph]] [Search INSPIRE].
[19] M. Sruthilaya, R. Mohanta, and S. Patra, Eur. Phys. J. C **78**, 719 (2018) [arXiv:1709.01737 [hep-ph]] [Search INSPIRE].
[20] A. E. Cárcamo Hernández, S. Kovalenko, J. W. F. Valle, and C. A. Vaquera-Araujo, J. High Energy Phys. **1707**, 118 (2017) [arXiv:1705.06320 [hep-ph]] [Search INSPIRE].
[21] D. Borah and B. Karmakar, Phys. Lett. B **789**, 59 (2019) [arXiv:1806.10685 [hep-ph]] [Search INSPIRE].
[22] A. E. Cárcamo Hernández and H. N. Long, J. Phys. G **45**, 045001 (2018) [arXiv:1705.05246 [hep-ph]] [Search INSPIRE].
[23] A. E. Cárcamo Hernández, H. N. Long, and V. V. Vien, Eur. Phys. J. C **78**, 804 (2018) [arXiv:1803.01636 [hep-ph]] [Search INSPIRE].
[24] A. E. Cárcamo Hernández, Y. Hidalgo Velásquez, and N. A. Pérez-Julve, Eur. Phys. J. C **79**, 828 (2019) [arXiv:1905.02323 [hep-ph]] [Search INSPIRE].
[25] A. E. Cárcamo Hernández and S. F. King, arXiv:1903.02565 [hep-ph] [Search INSPIRE].
[26] A. E. Cárcamo Hernández, S. Kovalenko, J. W. F. Valle, and C. A. Vaquera-Araujo, J. High Energy Phys. **1902**, 065 (2019) [arXiv:1811.03018 [hep-ph]] [Search INSPIRE].
[27] A. E. Cárcamo Hernández, J. Marchant González, and U. J. Saldaña-Salazar, Phys. Rev. D **100**, 035024 (2019) [arXiv:1904.09993 [hep-ph]] [Search INSPIRE].
[28] A. E. Cárcamo Hernández, N. A. Pérez-Julve, and Y. Hidalgo Velásquez, arXiv:1907.13083 [hep-ph] [Search INSPIRE].
[29] P. V. Dong, H. N. Long, C. H. Nam, and V. V. Vien, Phys. Rev. D **85**, 053001 (2012) [arXiv:1111.6360 [hep-ph]] [Search INSPIRE].
[30] K. Bora, Horizon **2**, 112 (2013) [arXiv:1206.5909 [hep-ph]] [Search INSPIRE].
[31] Z.-z. Xing, H. Zhang, and S. Zhou, Phys. Rev. D **77**, 113016 (2008) [arXiv:0712.1419 [hep-ph]] [Search INSPIRE].
[32] C. Patrignani et al. [Particle Data Group], Chin. Phys. C **40**, 100001 (2016).
[33] M. C. Gonzalez-Garcia, M. Maltoni, and T. Schwetz, J. High Energy Phys. **1411**, 052 (2014) [arXiv:1409.5439 [hep-ph]] [Search INSPIRE].
[34] M. Tegmark et al. [SDSS Collaboration], Phys. Rev. D **69**, 103501 (2004) [arXiv:astro-ph/0310723] [Search INSPIRE].
[35] P. A. R. Ade et al. [Planck Collaboration], Astron. Astrophys. **594**, A13 (2016) [arXiv:1502.01589 [astro-ph.CO]] [Search INSPIRE].
[36] L. Lavoura, Eur. Phys. J. C **29**, 191 (2003) [arXiv:hep-ph/0302221] [Search INSPIRE].
[37] L. T. Hue, L. D. Ninh, T. T. Thuc, and N. T. T. Dat, Eur. Phys. J. C **78**, 128 (2018) [arXiv:1708.09723 [hep-ph]] [Search INSPIRE].

[38] M. D. Campos, A. E. Cárcamo Hernández, H. Päs, and E. Schumacher, Phys. Rev. D **91**, 116011 (2015) [arXiv:1408.1652 [hep-ph]] [Search INSPIRE].
[39] M. Lindner, M. Platscher, and F. S. Queiroz, Phys. Rept. **731**, 1 (2018) [arXiv:1610.06587 [hep-ph]] [Search INSPIRE].